J NeuroEngineering Rehabil
https://doi.org/10.1186/s12984-026-01937-4
Article in Press

Exoskeleton frontal and sagittal plane hip torque improves propulsion and transient stability during walking in individuals with hemiparesis

Received: 18 June 2025
Accepted: 1 March 2026
Published online: 11 May 2026

Cite this article as: Archangeli D., Gunnell A., Winship O. *et al.* Exoskeleton frontal and sagittal plane hip torque improves propulsion and transient stability during walking in individuals with hemiparesis. *J NeuroEngineering Rehabil* (2026). https://doi.org/10.1186/s12984-026-01937-4

Dante Archangeli, Andrew Gunnell, Owen Winship, Yueshan Xiong, Lukas Gabert, Rosemarie Murray, Steven Edgley, K. Bo Foreman & Tommaso Lenzi

Title:

Exoskeleton Frontal and Sagittal Plane Hip Torque Improves Propulsion and Transient Stability during Walking in Individuals with Hemiparesis

Authors:

Dante Archangeli[1], Andrew Gunnell[1,2], Owen Winship[1], Yueshan Xiong[3], Lukas Gabert[1], Rosemarie Murray[1,2,*], Steven Edgley[4], K. Bo Foreman[5], Tommaso Lenzi[1,2,6]

Affiliations:

1. HGN Lab for Bionic Engineering, Department of Mechanical Engineering and Robotic Center, University of Utah, Salt Lake City, UT

2. Rocky Mountain Center for Occupational and Environmental Health, Salt Lake City, UT

3. Division of Public Health, Department of Family and Preventive Medicine, University of Utah, Salt Lake City, UT

4. Director of Stroke Rehabilitation, Craig H. Neilsen Rehabilitation Hospital, University of Utah, Salt Lake City, UT

5. Department of Physical Therapy & Athletic Training at the University of Utah, Salt Lake City, UT, 84108, USA

6. Department of Biomedical Engineering, University of Utah, Salt Lake City, UT

* corresponding author

Abstract

Background: Millions of people around the world experience post-stroke hemiparesis, making it difficult to move one side of the body. Hemiparesis impairs an individual's muscle strength and coordination which limits gait speed, efficiency, and endurance and contributes to reduced community participation. These limitations in strength and control also negatively impact balance, leading to a high prevalence of instability, falls, and fall-related injuries. Assistive technologies like powered exoskeletons that apply torques to the hips in the sagittal plane (hip flexion and extension) and frontal plane (hip abduction and adduction) may benefit both gait efficiency and stability in hemiparetic populations.

Methods: In this study, we investigate the impact of exoskeleton-delivered frontal and sagittal plane hip torque in eight individuals with hemiparesis. Participants completed two-minute walking bouts on an instrumented treadmill with no exoskeleton, and then with the exoskeleton applying phase-based flexion and extension assistance. They then completed a series of abduction torque trials, in which they walked with the exoskeleton-supplied sagittal-plane assistance for 10 strides, and then sagittal-plane assistance and constant abduction torque for 10 strides. The abduction torque series consisted of four levels of abduction torque, each repeated 5 times, in random order.

Results: Compared to steady-state walking without the exoskeleton, the application of sagittal plane torques significantly increased propulsive forces at push-off for the non-paretic limb by 0.83 ± 0.32% BW ($p = 0.0373$) and had little impact on step width or margin of stability. In the transient period following onset, hip abduction torques significantly increased step width by 0.053 ± 0.011 m (adjusted $p < 0.025$) and margin of stability for the paretic and non-paretic limb by 0.039 ± 0.006 m (adjusted $p < 0.025$) and 0.014 ± 0.004 m (adjusted $p = 0.01$), respectively. These outcomes are correlated with the level of abduction assistance.

Conclusion: These results provide initial evidence supporting the use of a hip exoskeleton to impact foot placement, margin of stability, and propulsion in individuals with hemiparesis, which may benefit both gait efficiency and stability.

Keywords Hemiparesis, Balance, Gait, Exoskeleton, Hip, Stroke, Mobility, Stability

Background

Each year, more than ten million individuals around the world suffer a stroke (1). Many of these individuals develop hemiparesis, which limits the strength and control of one side of the body (2,3). The resulting asymmetric gait is slower, less efficient, and less stable than the gait of healthy individuals (4–6). These limitations substantially increase the metabolic cost of transport and lead to an increased rate of falls and fall-related injury (7–10). Due in part to these limitations, individuals with hemiparesis have decreased community mobility, quality of life (11–13), and life expectancy (14). Improving the gait speed, efficiency, and stability of individuals with hemiparesis may have significant health benefits.

Walking speed and metabolic cost of transport of individuals with hemiparesis may improve by augmenting strength and power of the paretic limb in the sagittal plane. In hemiparetic populations, greater positive power generation of ankle plantarflexors and hip extensors (15) along with hip extensor strength (16) is linked to increased walking speed. Similarly, ankle plantarflexion and hip extension moments during the toe-off phase of the gait cycle generate an anterior ground reaction force that propels the body forward (i.e., propulsive force) (17–19). This anterior ground reaction force is directly related to forward motion of the body's center of mass and is correlated with walking speed in hemiparetic populations (20,21). Thus, augmenting the paretic limb strength, power, or anterior ground reaction force may increase walking speed. An increase in walking speed may also benefit the metabolic cost of hemiparetic gait. Hemiparetic walkers with faster self-selected walking speeds (2.5-4 km/h) use less metabolic energy per distance traveled than those with slower self-selected speeds (1-2.5 km/h)(22). Moreover, within individuals with hemiparesis, increasing gait speed decreases the metabolic costs of transport for (23,24). Thus, both walking speed and metabolic efficiency may be positively impacted by increasing the anterior ground reaction force through augmenting paretic limb strength or power.

Individuals with hemiparesis have poor medio-lateral balance (7). These individuals rely on the hip abductors and adductors to maintain equilibrium during dynamic and postural tasks

(25–27). By controlling the frontal-plane torque of the stance limb, individuals with hemiparesis can shift their center of mass with respect to their center of pressure to reduce torso sway and improve stability (28). Alternatively, frontal-plane torques applied by the hip of the swing leg control foot placement, which can impact stability during lateral stepping strategies (27,29). Unfortunately, individuals with hemiparesis have weakened hip muscles of the paretic limb (2,30) and longer reaction time following a perturbation (27,29). This lack of hip strength and control makes balance more challenging and may contribute to the high prevalence of falls in hemiparetic populations (7,8). In addition, individuals may compensate for the lack of hip strength on the paretic limb with increased demands on the non-paretic hip (29). Therefore, augmenting the strength and control of both hips in the frontal plane may improve stability.

Powered exoskeletons are an emerging technology that may improve hemiparetic gait efficiency and stability by using their actuators to augment the residual strength and coordination of the paretic limb. These devices use motors, batteries, and intelligent control algorithms to apply external forces and torques to aid joint motion. They can function as gait trainers to supplement existing physical therapy routines (31–35) or can be worn while performing an activity to augment an individual's baseline abilities (36). Recently, devices that generate sagittal plane torques to augment the ankle (37–39), knee (40), or hip (41–44) have made functional improvements in hemiparetic mobility. Notably, devices acting on just the paretic (44) or both the paretic and non-paretic hips (42,43) have increased stride length and walking speed, while devices acting at the ankle have decreased the metabolic cost of transport (37,39).

These studies indicate the potential for exoskeletons to improve gait speed and efficiency in hemiparetic populations, but that alone is not sufficient for clinical translation. Exoskeletons have yet to improve hemiparetic stability (45), which is critical for reintegration into the community following a stroke. However, growing evidence suggests that hip exoskeletons that act in the frontal plane can affect foot placement in healthy individuals, potentially improving stability. Hip exoskeletons that generate frontal-plane hip torque (abduction or adduction) can change step width (increase and decrease, respectively) in young adult populations during steady-state walking (46–48). Recent work in healthy individuals has also demonstrated that hip exoskeletons can generate frontal-plane torque to modulate step width during perturbed walking (49). These studies provide initial evidence that frontal-plane hip torques applied to healthy individuals can alter foot placement and may positively impact stability during steady-state and perturbed walking. However, previous studies have not yet established a relationship between the magnitude of frontal-plane torque and immediate changes in foot placement or measures of stability. This information is critical to developing control algorithms that intelligently apply hip torque to alter foot placement and reduce the risk of falls. Crucially, to the best of our knowledge, no studies have demonstrated the effectiveness of exoskeleton-mediated frontal-plane assistance in individuals with hemiparesis, who often respond differently to interventions than those without motor impairment. Therefore, it is unclear whether frontal-plane hip torques can increase lateral foot placement and margin of stability in individuals with hemiparesis.

The goal of this study was to explore the steady-state effect of phase-based flexion and extension assistance generated by a portable hip exoskeleton on hemiparetic walking, and the transient effects of adding a constant abduction torque to the sagittal-plane assistance. Our central hypothesis is that hip abduction torque will increase step width and margin of stability, while sagittal plane torques will increase propulsive force. To test this hypothesis, we measured the foot placement and full body kinematics and kinetics of individuals with hemiparesis while receiving hip torques applied by an exoskeleton and compared these results to the same subjects walking without the exoskeleton. We applied a sagittal-plane assistive torque profile and evaluated its effect on propulsive force during steady-state walking. We tested multiple levels of hip abduction torque to closely assess the relationship between frontal-plane torque and immediate changes in step width and margin of stability. As a secondary outcome, we quantified the change in the biological energy generated by the lower-limb joints. Quantifying the effect of hip assistance on gait stability and propulsion in individuals with hemiparesis could lead to the effective translation of interventions such as portable exoskeletons, which provide immediate benefits for this population by increasing mobility and quality of life.

Methods

A. Participants

We recruited eight individuals with hemiparesis (3 female, 5 male; body weight 75 ± 7.5 kg; age 47 ± 18 years; height 1.71 ± 0.066 m; mean ± standard deviation, see Table 1). Participant inclusion criteria included the following: age between 18 and 85 years, hemiparesis for at least 6 months since onset, and the ability to walk on a treadmill for 6 minutes. Participants were excluded from the study if they were over 250 lbs., had a cognitive deficiency that precluded the ability to give informed consent, were pregnant, or had a co-morbidity that interfered with the study. All subjects were at least 5 years post-stroke. Four subjects had hemiparesis of the left limb, while the other four had hemiparesis of the right limb. The study was conducted with the approval of the Institutional Review Board of the University of Utah (Utah IRB #120712). All subjects provided informed consent and consented to the dissemination of pictures and videos.

B. Exoskeleton Device

Subjects in this study wore a bilateral hip exoskeleton (Fig. 1 a, b) that generates hip flexion and extension (sagittal-plane) torque, and hip abduction and adduction (frontal-plane) torque (46,50). The exoskeleton weighs 5.9 kg and leverages a parallel mechanism to generate up to 30 Nm of torque in both the frontal and sagittal planes. Each hip actuator is connected proximal to the user’s hips via a pelvis interface that consists of a lumbar wrap (Ottobock) and rigid, 3D-printed bars. These bars transfer forces and torques generated by the exoskeleton to the user’s torso and pelvis. The actuators are connected to the thigh through a cuff with passive degrees of freedom (51) to improve comfort and reduce spurious forces and torques (52,53). The exoskeleton controller generates Gaussian-shaped flexion and extension torques and a constant abduction torque. As described in previous work, two adaptive frequency oscillators independently estimate the cadence from each leg's thigh angle (51) The peak hip flexion angle is considered the start of the gait cycle. This method has demonstrated an error of less than 2%

in the gait phase estimate (51). The sagittal-plane assistance comprises a flexion torque Gaussian profile and an extension torque Gaussian profile, each independently controlled for each side. The experimenters tuned the magnitude, width, and timing of these torque profiles to each subject. The experimenter adjusted these parameters to maximize the exoskeleton power based on the online estimates observed in the GUI. The hip abduction torque was applied continuously. Data from the exoskeleton device was recorded at 500 Hz. Additional information regarding the design and control of the device can be found in prior work (46). Performance metrics for the exoskeleton are reported in the Supplementary Material (Fig. S 1).

C. Motion Capture Volume

Subjects in this study walked on a split-belt instrumented treadmill with instrumented handrails (Bertec Fit 5) within a 12-camera Vicon motion capture volume (Vicon Motion Systems, Centennial, CO, USA). We placed retroreflective markers (14 mm diameter, Vicon Motion Systems, Centennial, CO, USA) on the study participants, following a modified Plug-in-Gait marker set (54). This marker set included additional thigh and shank markers to improve tracking performance. Since the exoskeleton obscured the greater trochanter, we removed this marker from the set (Fig. 1a). No markers were placed on any moving parts of the exoskeleton. Prior to capturing experimental data, the subjects performed a static calibration pose (Vicon Nexus 2.1, Vicon Motion Systems, Centennial, CO) and a dynamic calibration motion (SCORE and SARA) to localize the hip and knee joint centers (55,56). Marker trajectories were recorded at 200 Hz while force and torque data from the instrumented treadmill and handrails were recorded at 1000 Hz.

D. Protocol

At the start of the experiment, the subjects changed into tightly fitted clothing and donned a safety harness to prevent falls. Retroreflective markers were placed, and the motion capture calibration routines were performed. The subjects walked on the split-belt instrumented treadmill for a few minutes while the speed gradually increased until they identified their comfortable walking speed. We recorded subjects' walking baselines at this comfortable speed for 2 minutes (*No Exoskeleton* condition, see supplementary video, Additional File 1).

Each subject then donned the bilateral exoskeleton for a short tuning session. The subject walked at their comfortable speed while the experimenter adjusted the timing and width of the sagittal plane torque profile for first the non-paretic and then the paretic limb. The experimenter adjusted these parameters to maximize a live estimate of the exoskeleton positive power, as positive power from a hip exoskeleton is associated with reduced energy expenditure from the biological hip (57). The experimenter then increased the magnitude of the peak torque from a starting value of 5 Nm until the participant began to develop a marching gait. The average peak torque magnitudes varied from 0.07 Nm/kg to 0.11 Nm/kg. Once an appropriate sagittal plane tuning was identified, the subject rested briefly before performing the motion capture calibration routines with the exoskeletons.

We then recorded the subject walking with the exoskeleton sagittal plane torque, along with five levels of abduction torque: 0 Nm/kg (Sagittal Only), 0.05 Nm/kg (Low), 0.083 Nm/kg (Medium), 0.117 Nm/kg (High), and 0.15 Nm/kg (Very High) (Fig. 1, supplementary video, Additional File 1). The abduction torque profile was selected through pilot testing with a

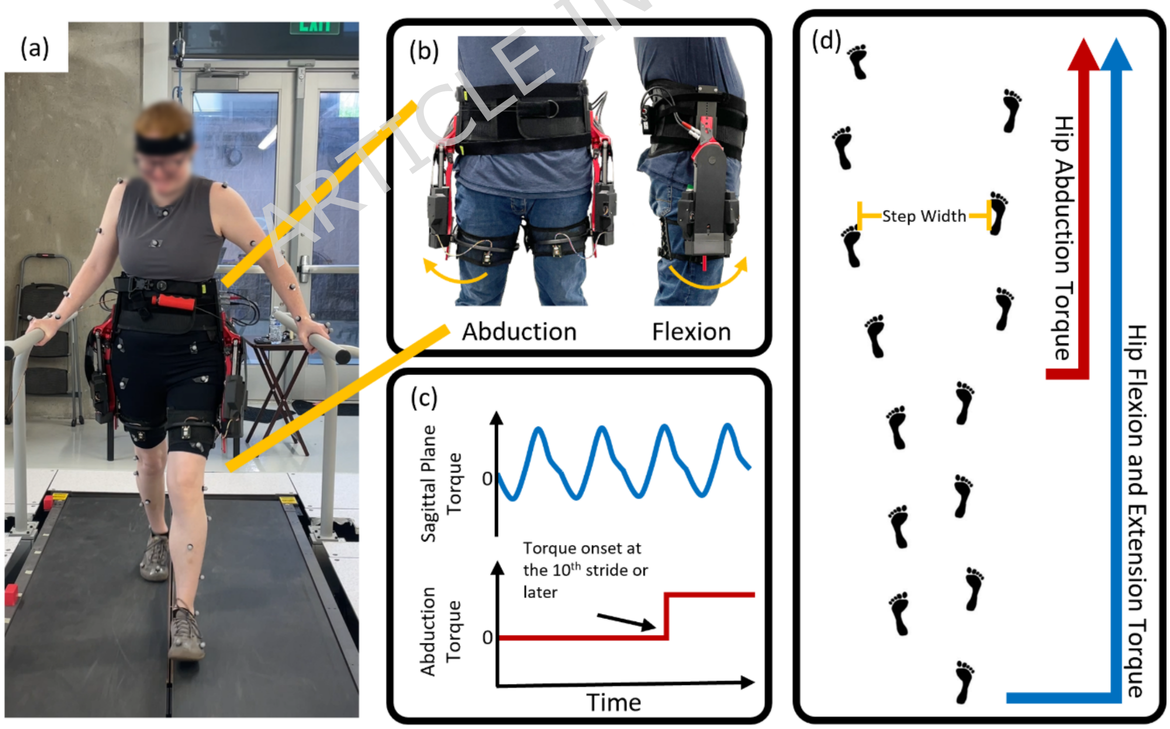

Fig. 1 (a) Eight individuals with hemiparesis walked on an instrumented treadmill with and without a bilateral hip exoskeleton. (b) The exoskeleton generates hip flexion and extension torque and abduction and adduction torque. (c) The exoskeleton applied flexion and extension torques to assist gait motion for every stride. Hip abduction torque was applied starting after the 10th stride and set to a constant level. (d) Exoskeleton torque resulted in changes in the kinematics and kinetics of the

S8	59	M	77.9	1.73	Hemorrhagic	15	L	0.9

* Functional Ambulation Category (FAC), †Ankle-Foot Orthosis (AFO), ‡Traumatic Brain Injury (TBI)

hemiparetic individual, in which a constant bilateral abduction torque profile produced greater changes in step width than Gaussian abduction torque profiles centered on either stance or swing phase, or a constant abduction stiffness profile. The maximum abduction torque was based on the participant's subjective comfort during pilot testing, and the number of levels was chosen to establish a dose-response relationship between abduction torque and step width. In all conditions, the subject walked at their comfortable speed for at least 3 minutes. The subject began each trial receiving only sagittal-plane torque. After at least 10 strides, the exoskeleton applied a constant bilateral abduction torque which initially turned on at 85% of the gait cycle of the non-paretic limb (mid-swing phase, Fig. 1 c). The subjects continued walking for at least 10 strides while the exoskeleton applied both sagittal-plane torque and the constant frontal-plane torque. Subjects were not warned when the abduction torque would begin, and the order of appearance of the abduction conditions was pseudo-randomized. Each of the Low to Very High conditions was tested at least five times to reliably capture the immediate response to frontal-plane assistance.

As many participants had limited experience walking on a treadmill, they were instructed to lightly hold the instrumented handrails. We recorded handrail forces in x, y, and z directions to compare reliance on the handrails across experimental conditions. Subjects who could not hold the handrail with their paretic hand wore a sling to prevent their hand from hitting the motion capture markers. Subjects were instructed to walk normally in all conditions.

E. Data Processing

For each subject and trial, recorded marker trajectories, ground reaction forces and torques, and handrail forces were filtered at 6 Hz (58). The forces and exoskeleton data were down-sampled to match the frequency of the markers at 200 Hz. Joint positions and torques were calculated in Visual 3D and imported into MATLAB. Joint power was calculated by multiplying the joint velocity in the respective plane by the corresponding joint torque. Similar to prior work (59–61), the *biological* hip torque and power were defined as the hip torque and power directly calculated from Visual 3D minus the *exoskeleton* torque and power, respectively.

Data for the paretic and non-paretic limb and exoskeleton actuators were segmented by the corresponding heel strikes and transformed to the gait phase domain. We extracted the last 50 strides of the No Exoskeleton and Sagittal conditions, along with the first 10 strides following abduction torque onset from each of the five trials for the Low to Very High conditions. We focused our analysis on this period to understand the potential to immediately impact step width and margin of stability, which may benefit stability and reduce the chance of falls in hemiparetic populations. To reduce the impact of handrail use on the outcome measures, a threshold was set as the magnitude of the mean non-paretic handrail force during the No Exoskeleton trial plus 5% of the magnitude of the subject’s body weight (i.e., the weight of an individual’s arm (62)). For the exoskeleton conditions, strides with a mean magnitude of the handrail resultant force exceeding the threshold magnitude were removed from the data analysis. Additionally, strides containing crossover steps were removed from the kinetic analysis. We extracted the primary outcome measures and kinematic and kinetic data from the remaining strides.

The primary outcome measures are the average step width during double support (47,63), the average paretic and non-paretic margin of stability during double support (64), and the maximum anterior ground reaction force for the paretic and non-paretic limbs (20) (Fig. 1 d). The maximum anterior ground reaction force was chosen as the primary propulsion metric because it is the metric most strongly associated with walking speed in post-stroke individuals (20). These metrics were calculated for each stride and then averaged across strides for each subject and condition. In this analysis, the paretic margin of stability was calculated during the double support phase immediately following paretic heel strike. In contrast, the non-paretic margin of stability corresponded to the second double support phase following paretic heel strike. Margin of stability was calculated as the distance between the extrapolated center of mass and the most lateral foot marker of the corresponding limb (e.g., paretic foot marker for paretic margin of stability) (64). Step width was calculated as the lateral distance between the heel markers (47,63). Extrapolated COM (xCOM) displacement was calculated as the difference between the maximum and minimum values of the lateral component of the xCOM during double support.

Kinematic and kinetic measures reported in the gait-phase domain were constructed from averaging the strides for each condition, subject, and limb. These averages were then pooled across subjects to construct group averages and standard errors for each condition. Similar to the primary outcomes, kinematic and kinetic measures for secondary outcomes were calculated per stride and then averaged per condition, subject, and limb. The total limb energy was calculated by adding together the total positive energy across the gait cycle of the hip in the frontal and sagittal planes, the knee in the sagittal plane, and the ankle in the sagittal plane. The trailing limb angle was calculated as the angle between a line extending from the pelvis center of mass to the fifth metatarsal at the moment of peak anterior ground reaction force (65).

F. Statistics

Statistical analysis of primary and secondary outcomes was conducted in Matlab (MathWorks). For steady state outcomes (paretic and non-paretic propulsion), we used paired *t*-tests to compare the sagittal plane assistance to the No Exoskeleton condition. For the transient outcomes (step width, paretic and non-paretic margin of stability), we used a mixed effects linear model with random intercept to compare statistical differences between the sagittal plane assistance condition and each of the other five conditions, similar to prior work (60,66,67). This model correctly accounted for the repeated measures of each subject due to the different experimental conditions. In the mixed effects models, the six conditions were included in the model as a categorical variable. Comparing the sagittal assistance condition to each of the other conditions resulted in 5 comparisons, after which the P values were adjusted following the Holm method (68). For transient outcomes, a second mixed effects linear model with random intercept was fit to the five exoskeleton conditions, with condition treated as a continuous variable equal to the level of abduction torque, which varied from 0.0 Nm/kg (Sagittal condition) to 0.15 Nm/kg (Very High condition). We report the linear model. The sample size was determined using a statistical power analysis based on pilot tests that estimated the change in step width caused by frontal-plane exoskeleton torque.

To quantify the speed of the human reaction, we analyzed the number of reactive heel strikes (i.e., steps) necessary to reach a statistically significant increase in step width for the four exoskeleton conditions with abduction torque greater than zero (i.e., Low to Very High conditions) following the Cumulative Sum Control Chart (i.e., *CuSum*) method (47,69,70). This method used the 20 steps prior to the application of frontal-plane torque to determine a baseline and standard deviation for the step width from which significant variations could be determined. Like prior work, we set the control limit to 3 standard deviations and the mean shift to 1 (47). We also reported the number of steps necessary to achieve the steady state (i.e., mean value) in step width after the application of abduction torque. These metrics were performed per subject, condition, and trial, and then averaged to create a mean and standard error estimate for each condition. These two tests were performed on subjects who were able to achieve a steady state response different from their baseline.

Descriptive statistics are provided for additional kinematic and kinetic outcomes. Among others, these included measures of hip torque in the frontal and sagittal planes, joint energy, stance knee flexion, and stance knee extension moment. All reported primary and secondary outcomes are presented as mean ± standard error unless otherwise stated.

Results

A. Propulsion

Fig. 2 shows the effect of steady-state sagittal-plane assistance on the non-paretic and paretic propulsion and trailing limb angle. Sagittal-plane assistance significantly increased non-paretic propulsion from 14.5 ± 1.6 % BW to 15.4 ± 1.8 % BW ($p = 0.0373$). Paretic propulsion did not significantly change between the No Exoskeleton (7.95 ± 1.3 % BW) and Sagittal (8.62 ± 1.5 % BW) conditions. The trailing limb angle increased slightly with the sagittal-plane assistance. Non-paretic trailing limb angle increased from 13.8 ± 2.1° in the No Exoskeleton condition to 14.3 ± 1.8° in the Sagittal condition. Paretic trailing limb angle increased slightly more, from 7.5 ± 2.6° to 8.3 ± 2.6°.

B. Transient Response

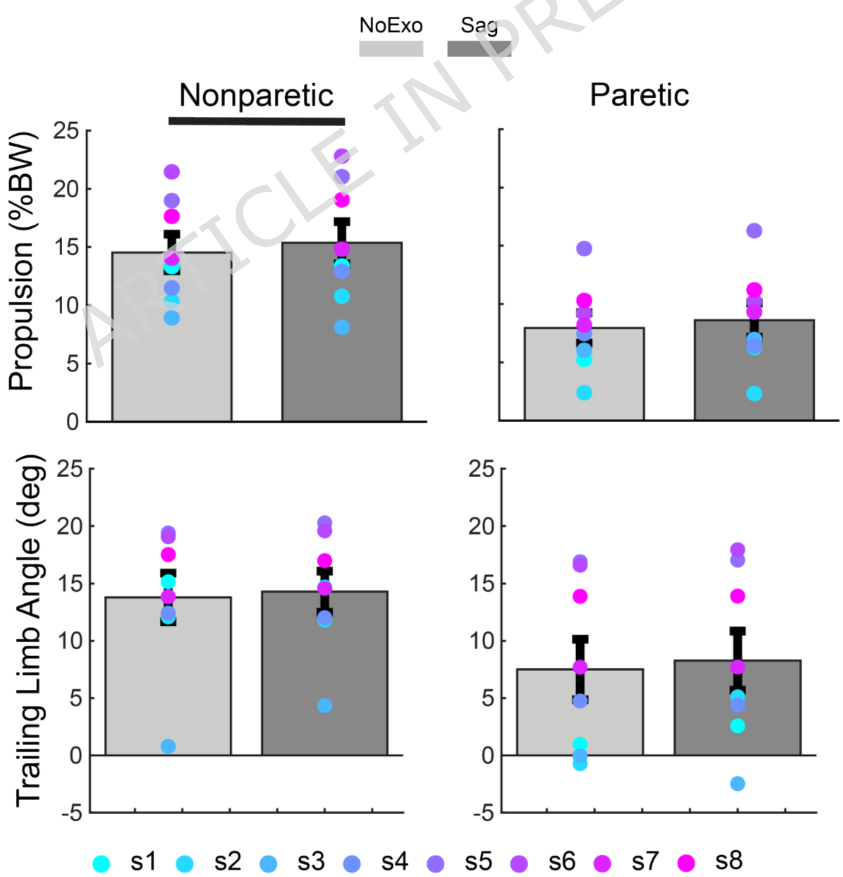

Fig. 2 (Top) Peak propulsion on the non-paretic (left) and paretic (right) limbs. (Bottom) Trailing limb angle for the nonparetic (left) and paretic (right) limbs. The plots show condition means (bars), standard error (error bars), and subject means (dots). Significant differences ($\alpha = 0.05$) are shown in

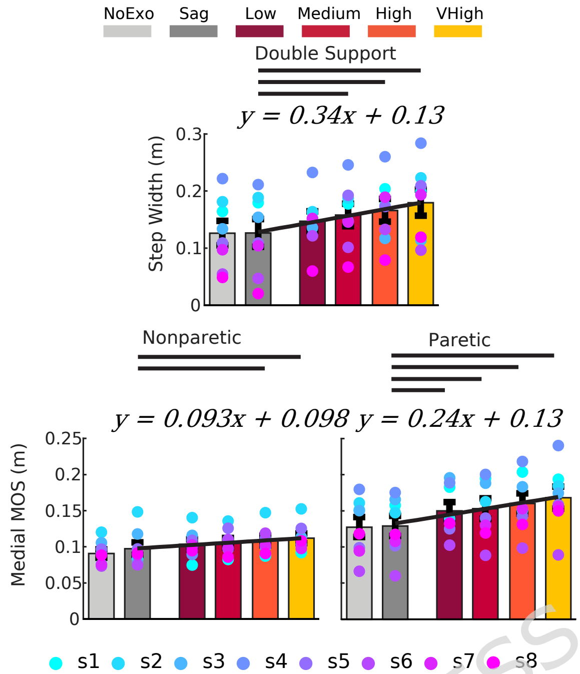

Fig. 4 The mean, standard error, and subject mean for the step width, margin of stability (MoS). Significant differences ($\alpha = 0.05$) are shown in black horizontal lines. Relationships between abduction torque and outcome measure were fit with a linear mixed effect model with random intercept.

Analysis of the transient behavior for step width indicates that changes in the step width occur rapidly after the application of abduction torque (Fig. 3). Abduction torque was applied after the 10th stride (i.e., 20th step) and led to a rapid increase in step width. Following prior work (47), the minimum number of steps necessary to elicit a significant change from baseline for the Low, Medium, High, and Very High conditions are 3.18 ± 0.23, 2.79 ± 0.22, 2.74 ± 0.20, and 2.34 ± 0.16 indicating that significant increases in step width occurred faster at higher levels of abduction torque. The mean number of steps needed to achieve the mean change for the step width for the Low, Medium, High, and Very High conditions is 2.48 ± 0.10, 3.16 ± 0.39, 3.22 ± 0.37, and 2.88 ± 0.39 (mean step ± standard error) which suggests that more steps may be needed to reach the mean change in step width during Medium and High conditions.

Based on these results, we analyzed the change in step width and margin of stability in the first three strides following the application of frontal-plane torque. The primary outcome measures of this study (step width, paretic and non-paretic margin of stability) were smallest in the No Exoskeleton condition (0.126 ± 0.022 m, 0.127 ± 0.014 m, and 0.091 ± 0.006 m, respectively) (Fig. 4). None of these outcome measures significantly changed between the No Exoskeleton and Sagittal conditions. The outcome measures reached their highest values in the Very High condition (step width: 0.180 ± 0.023 m; paretic margin of stability: 0.168 ± 0.015 m; non-paretic margin of stability: 0.112 ± 0.007 m). Step width significantly increased from the Sagittal condition to the Medium and above abduction torque levels. Paretic margin of stability significantly increased from the Sagittal condition to the Low and above abduction torque levels. Non-paretic margin of stability significantly increased from the Sagittal condition to the High and above abduction torque levels. The step width and paretic and non-paretic margin of stability showed the largest increase between the No Exoskeleton and the Very High condition (0.061 ± 0.011 m, 0.040 ± 0.006 m, 0.024 ± 0.004 m, respectively; mean difference ± standard error; adjusted $p < 0.001$).

On average, the step width, paretic and non-paretic margin of stability, and non-paretic propulsion significantly increased with increasing abduction assistance. These outcomes are linearly correlated with the level of abduction torque. The slope and intercept corresponding to the fixed effects of the linear mixed effects model are reported in Fig. 4.

C. Kinematic and Kinetic Measures

Kinematics and kinetics for the hip are shown in Fig. 5 and for the ankle and knee joints in Fig. 6. A qualitative description of the hip, knee, and ankle kinematics and kinetics is reported in the text below. Additional descriptive statistics are provided for the joints in the supplementary materials (Table S III, Table S IV).

The mean frontal-plane hip angle decreased between the No Exoskeleton and Very High condition (Fig. 5). The magnitude of the biologic abduction hip moment was similar between the No Exoskeleton and Sagittal conditions and decreased with increasing exoskeleton abduction torque. In contrast, the frontal-plane energy injected by the biological hip (i.e. integral of positive power) increased from the No Exoskeleton to Sagittal conditions but decreased with abduction torque, reaching the lowest value in the Very High condition.

In the sagittal plane, maximum flexion and extension angles for the hip remain relatively unchanged across the six conditions. In contrast, the biologic hip extension torque for both the paretic and non-paretic limbs was largest in the No Exoskeleton condition, decreased in the Sagittal condition, and was lowest for the paretic limb in the Very High condition, and for the non-paretic limb in the Low condition. The biologic hip flexion torque was highest in the Sagittal condition and lowest for the paretic limb in the Very High condition and for the non-paretic limb in the Medium condition. A notable decrease in the biologic moment and power occurs between the No Exoskeleton and the five exoskeleton conditions (i.e., Sagittal to Very High condition) at

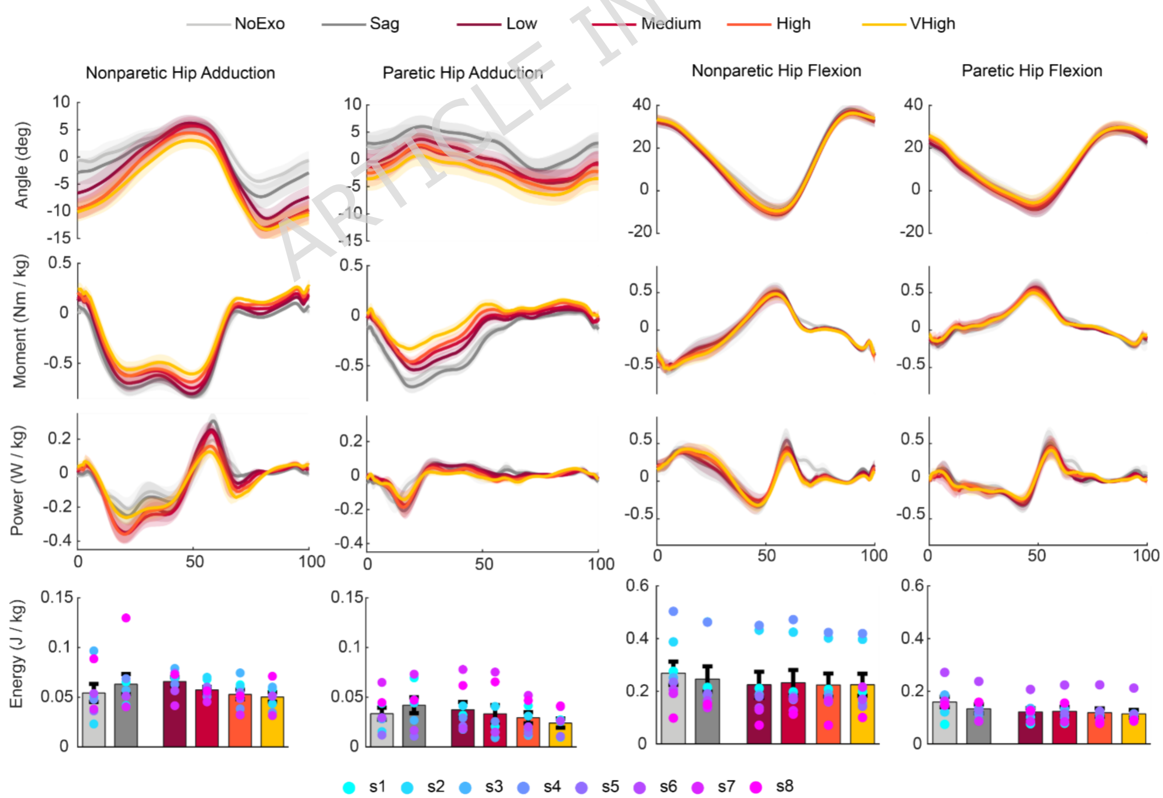

Fig. 5 Hip angle, moment, power, and positive energy for the paretic and non-paretic limb, segmented heel strike to heel strike. Adduction and flexion angle and moment are positive. The plots show condition means (solid lines or bars), standard error (shaded regions or error bars), and subject means (dots).

about 60-80% of the gait cycle, which is likely caused by the application of exoskeleton flexion torque. The energy injected by the biological hip in the sagittal plane decreased from the No Exoskeleton to Sagittal conditions and was lowest in the Very High.

Kinematics and kinetics for the paretic and non-paretic knee in the sagittal plane are shown in Fig. 6. Notably, stance knee flexion (i.e., knee flexion during the first half of the gait cycle) increases from No Exoskeleton to the Very High condition for both the paretic and non-paretic limb. The increase in stance knee flexion is mirrored by an increase in extension moment occurring at the same time. The energy injected by the paretic and non-paretic knee increased from No Exoskeleton to the Sagittal condition and was relatively constant for the remaining conditions. Across the six conditions, the maximum plantarflexion and dorsiflexion angles remain relatively unchanged. The maximum plantarflexion moment for the paretic and non-paretic ankle increased slightly from the No Exoskeleton condition to the five exoskeleton conditions. The non-paretic peak ankle power slightly increased from the No Exoskeleton

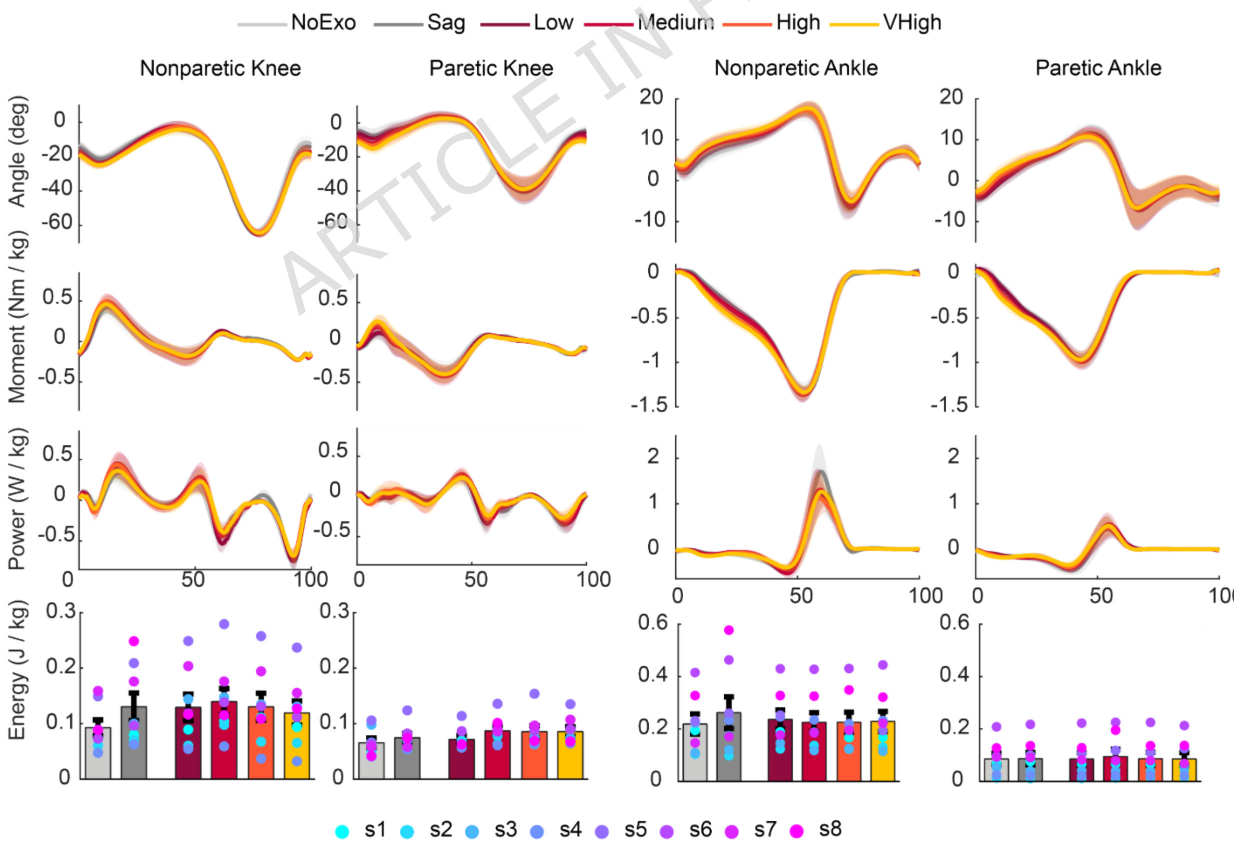

Fig. 6 Sagittal-plane ankle and knee angle, moment, power, and positive energy for the paretic and non-paretic limb, segmented heel strike to heel strike. Ankle dorsiflexion and knee extension angle and moment are positive. The plots show condition means (solid lines or bars), standard error (shaded

condition to the Sagittal condition. Similarly, the energy injected by the non-paretic ankle increased from the No Exoskeleton condition to the Sagittal condition. Paretic ankle power and energy remained consistent across conditions.

The biologic energy injected by the paretic and non-paretic limb (i.e., integral of positive power) varied with exoskeleton assistance (Table S III, Table S IV). The paretic limb biologic energy injection was similar between the No Exoskeleton and Sagittal condition (0.343 ± 0.041 J/kg and 0.336 ± 0.038, respectively) and lowest in the Very High condition (0.309 ± 0.040 J/kg). The non-paretic biologic energy injection increased between the No Exoskeleton and Sagittal condition (0.634 ± 0.036 J/kg and 0.702 ± 0.073 J/kg, respectively) but was lowest in the Very High condition (0.622 ± 0.035 J/kg).

The center of mass and extrapolated center of mass displacement decreased from the No Exoskeleton to the Sagittal condition (Fig. 7). The application of frontal-plane torque slightly increased the center of mass displacement from the No Exoskeleton condition to the Very High condition which was more pronounced in the extrapolated center of mass.

Discussion

Exoskeletons are emerging technologies with the potential to improve mobility for hundreds of millions of individuals with physical disability. In this paper, we explore the impact of sagittal and frontal-plane hip torques applied by a bilateral exoskeleton on individuals with hemiparesis.

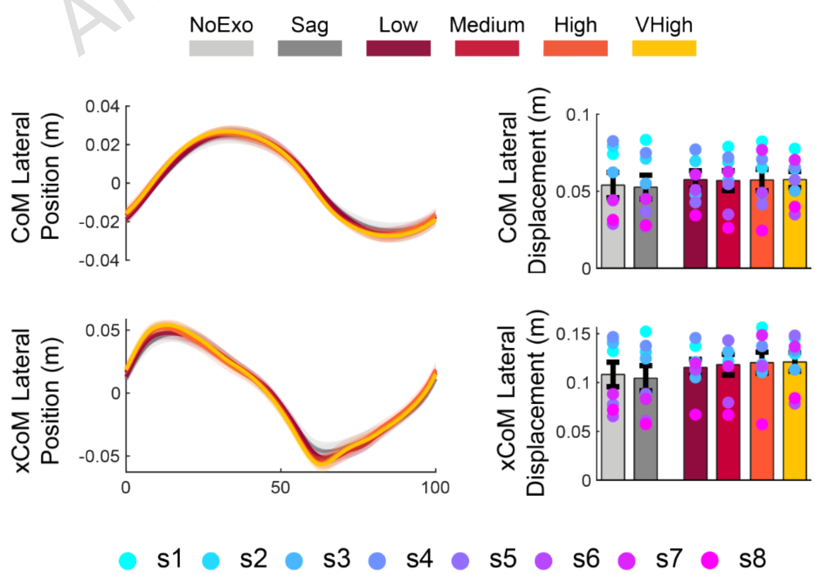

Fig. 7 (Left) The mediolateral position of the center of mass (CoM) and extrapolated center of mass (xCoM) across the gait cycle, segmented by the paretic limb heel strike. (Right) The mediolateral displacement of the CoM and xCoM. The plots show condition means (solid lines or bars), standard

Our results show that applying sagittal hip assistance torques with a portable exoskeleton significantly increased the propulsive force at push-off for the non-paretic limb, but not the paretic limb. Applying hip abduction torque significantly increased the step width and the paretic and non-paretic margin of stability (adjusted $p < 0.05$), and these outcomes correlate linearly with the magnitude of the torque. Cumulatively, the results of this study show, for the first time, that a portable hip exoskeleton can change step width while improving propulsion. Increasing step-width may improve stability against lateral perturbations, while improving propulsion may result in increased walking speed (42) and reduced metabolic effort (39).

Step width and margin of stability are key indicators of balance and stability (71,72). These metrics change significantly with age (73), mobility disorders (74–77), and during a perturbation (78,79). At baseline, the mean and standard error of the step width were similar to normative data for individuals with hemiparesis(77). As with prior work with non-paretic populations (49,61,80), we demonstrate that applying sagittal-plane hip torques does not significantly change the step width Fig. 4. In contrast, applying hip abduction torque significantly increases the step width from the Sagittal condition to the Medium, High, and Very High abduction torque conditions. Margin of stability increased for both the paretic and non-paretic limb, indicating increased resistance to perturbation impulses from either direction. Furthermore, a mixed effects linear model indicates that step width and margin of stability are positively correlated with the level of applied abduction torque. This observation contrasts with prior studies using a bilateral exoskeleton with an admittance controller, which found that step width tended to reach a plateau at high stiffness levels (47). However, a direct comparison is difficult due to the subject population and the inability to compare admittance stiffness to abduction torque. The linear relationship identified in this work links the magnitude of hip abduction torques generated by an exoskeleton to critical stability measures, informing the design and control of exoskeletons intended for balance augmentation.

The increase in step width resulting from abduction torques is consistent with experiments on healthy controls that applied the torque throughout the gait cycle or only during the swing phase, which reported changes in step width of approximately 0.05-0.08 m (47,49,50). In contrast, studies exploring the application of abduction torque during only the stance phase had inconsistent effects on step width (46) and reduced the margin of stability (81). The decrease in margin of stability found in healthy populations may be related to an increase in center of mass displacement with little to no increase in step width, which differs from this study which indicated that continuously applied abduction torques lead to large increases in step width compared to relatively small changes in center of mass excursion (Fig. 4, Fig. 7). These comparisons, though confounded by the subject populations, indicate that the timing of exoskeleton abduction torque may influence its effect on both step width and margin of stability.

Changes in the paretic and non-paretic margins of stability likely result from differences in the step width. The step width during double support was similar between the No Exoskeleton and Sagittal conditions (0.126 ± 0.022 m compared to 0.127 ± 0.024 m) and increased with increasing abduction torque (Fig. 4**Error! Reference source not found.**). The largest increase from the No Exoskeleton condition was 0.061 ± 0.011 m and occurred in the Very High condition. The extrapolated center of mass displacement also increased with abduction assistance, though to a lesser extent (maximum increase of 0.016 ± 0.011 m from No Exoskeleton) (Fig. 7). Thus, increases in step width and by extension, the base of support, are likely the primary contributor to the increases in margin of stability rather than decreases in center of mass motion. Future work should evaluate whether an exoskeleton can improve the margin of stability by reducing the extrapolated center-of-mass displacement in hemiparetic individuals and compare that with step-width increases.

Step width changes relatively quickly following the application of abduction torques. On average, these changes begin during the stride in which the abduction assistance is applied and are statistically different from baseline within four steps or less, which matches prior work with healthy controls (47) (Fig. 3). The average number of reactive heel strikes necessary to elicit a change in the outcome measures was 3.18 ± 0.23 for the Low condition and 2.34 ± 0.15 for the Very High, indicating that larger torque tended to cause a faster change in outcome measures. In contrast, the number of steps necessary to achieve the mean change in outcome measure increased from the Low condition (2.48 ± 0.10) to the Very High Condition (2.88 ± 0.39), indicating that, while changes in step width may have occurred faster at larger levels of assistance, the increase in step width meant that it took longer to achieve the mean value. While step width increases with abduction assistance, further studies are needed to determine whether this increase is sufficient to improve stability and balance in response to perturbations. Studies with hemiparetic and healthy populations indicate that lateral perturbations increase step width by about 0.05 m and margin of stability by 0.006 m to 0.012 m (78,79). In this study, the increase in step width from the No Exoskeleton condition exceeded 0.05 m in the Very High condition, while the increase in margin of stability exceeded 0.012 m in the Medium, High, and Very High conditions. However, in this study, subjects performed unperturbed walking and were not instructed to modify their gait in response to exoskeleton applied torque. Thus, future studies must determine whether changes in step width and margin of stability are faster or greater when subjects receive coaching or exoskeleton assistance during perturbation. Although this work indicates that abduction torques can impact margin of stability in hemiparetic gait, the increase in margin of stability should be interpreted only as an increase in the instantaneous mechanical stability of the subjects, not an improvement in their physiological ability to modulate their balance. By determining the abduction torque required to increase step width, these results can inform the design of future reactive controllers that aim to strategically enhance the mechanical stability of hemiparetic users, for example, right after a lateral perturbation occurs.

Propulsive force during late stance increases walking speed and efficiency in hemiparetic populations. The propulsive force propels the center of mass forward during level walking and is influenced by the ankle plantarflexion and hip flexion (17–19). Studies with hemiparetic populations indicate that walking speed is correlated with propulsive force (21). Moreover, the use of a bilateral hip exoskeleton in hemiparetic populations increased walking speed and propulsion (42) while a unilateral ankle exoskeleton improved metabolic cost of walking and the paretic limb propulsion (39). At baseline, the magnitude and variability of the paretic and non-paretic propulsion of our participants were roughly in line with previous studies (39,42). The application of sagittal-plane hip torques significantly increased the propulsive force (i.e., anterior ground reaction force) between the No Exoskeleton and Sagittal condition for the non-paretic limb (i.e., 14.5 ± 1.6% BW to 15.4 ± 1.8 % BW, 5.6% increase, p = 0.0373) (Fig. 2). The increase in non-paretic limb propulsive force between the Sagittal and No Exoskeleton condition (0.81% BW) matches the largest increase found using a bilateral hip exoskeleton (0.75% to 0.99% BW) (42). The propulsive force also increased for the paretic limb, but the difference was not significant (i.e., 8.0 ± 1.3% BW to 8.6 ± 1.5 % BW, 8.4% increase, p = 0.0573). This change falls within the range found using a bilateral hip exoskeleton (increase of 0.60%-1.25% BW)(42). The effect of sagittal-plane assistance on paretic limb propulsion may have been confounded by the effect of ankle-foot orthoses (AFOs) worn on the paretic ankle by two of the participants. While participants without AFOs experienced a mean increase in paretic limb propulsion of 1.1 ± 0.1% BW, the two participants wearing AFOs experienced a decrease in paretic limb propulsion of 0.06 and 1.1% BW. The AFO's restriction on ankle motion, or the specific motor deficits that necessitate its use, may influence participants' ability to convert hip assistance into propulsive force at the foot. On the other hand, increase in paretic limb propulsion among non-AFO users approaches the increase found using a unilateral ankle exoskeleton (increase of 1.27% BW) (39), which suggests it may be a viable alternative for this population. For both the paretic and non-paretic limbs, the increase in propulsion may be explained by the increase trailing limb angle, as prior work posits (65). Previous work with exoskeletons that improve propulsion has also improved walking speed (42) and metabolic cost (39) in hemiparetic populations, suggesting that the current exoskeleton may also benefits hemiparetic gait speed and efficiency.

Decreased positive energy and power generated by the biological lower-limb joints have been linked to increased walking efficiency. Studies with ankle and hip exoskeletons indicate that a reduction in the positive biological energy (i.e., integral of positive power) or power per stride can lead to a reduction in the metabolic cost of transport in adults and clinical populations (61,82,83). On the paretic side, we found that the total limb energy decreased in response to sagittal plane assistance, primarily driven by a reduction in hip energy in the sagittal plane. On the non-paretic side, sagittal plane assistance again reduced hip energy in the sagittal plane.

However, we also observed an increase in positive energy at the ankle joint, which offset the reduction in hip energy. As a result, the total limb energy increased on the non-paretic side. The observed difference in ankle energy between the two limbs may be responsible for the difference in limb propulsion, which increases on the non-paretic side, but not on the paretic side. Interestingly, when the exoskeleton provides frontal-plane torque in addition to sagittal-plane torque, the total biological energy of both limbs decreases, largely due to the reduction in frontal-plane hip energy which decreases by 0.018 J/kg on the paretic side and 0.013 J/kg on the non-paretic side. As a result, when comparing the No Exoskeleton condition to the Very High abduction torque condition, the paretic total biological limb energy decreased from 0.343 ±0.041 J/kg to 0.309 ±0.040 J/kg, while the non-paretic total biological limb energy remained about the same, at 0.634 ±0.036 J/kg and 0.622 ±0.035 J/kg, respectively. By concurrently increasing propulsion and reducing positive biological limb energy, an exoskeleton that applies both frontal- and sagittal-plane hip torques could improve the metabolic efficiency of individuals with paresis. Future studies should directly measure metabolic cost to test this hypothesis.

Individuals with hemiparesis have weakened muscles of their paretic limb (2,3,30) which may negatively impact balance and gait efficiency. Exoskeletons used for rehabilitation often aim to increase muscle strength. In contrast, exoskeletons used for mobility assistance, like the one used in this study, can improve performance through amplifying a user’s ability. In this study, exoskeleton hip torques decreased the peak biologic moment of the paretic and non-paretic hip in the frontal and sagittal planes (Fig. 5, Fig. 6, Table S III, Table S IV). Because these changes occurred while walking at the same gait speed, they suggest that a hip exoskeleton may be able to increase the user’s walking endurance, the total walking distance, or the maximum walking speed.

Individuals with hemiparesis often suffer from knee hyperextension which may lead to knee injury and pain (84–86). Prior work with hemiparetic individuals showed that gait training with an exoskeleton that generated hip flexion torques during that stance phase of walking lead to decreases in knee hyperextension (35). In contrast, this study suggests that the simultaneous application of hip extension torque and hip abduction torque can increase stance knee flexion

(Fig. 6, Table S III) while also increasing propulsion. Moreover, maximum knee extension decreases with increasing abduction torque (Table S III). Thus, the application of hip abduction torques should be considered when aiming to decrease knee hyperextension.

Limitations

In this study, abduction torque was added to the sagittal-plane assistance, as we envision real-world hip exoskeletons continuously supplying sagittal-plane torque to improve walking speed (42–44) and possibly reduce effort, and discontinuously supplying frontal-plane torque to improve response to perturbations. As a result, this study was not able to assess the impact of device weight or the effect of pure abduction torque on hemiparetic gait. Based on current exoskeleton literature, we expect that the added exoskeleton weight would increase the metabolic cost of walking with minimal effects on gait kinematics.

Individuals with hemiparesis are a heterogeneous group, and responses to a given intervention may vary with their specific presentation. We did not assess participants' motor impairment, muscle strength, spasticity, or joint range of motion out of concern that additional experimental time would fatigue participants. However, these metrics would provide deeper insights into how hemiparetic presentation affects the response to exoskeleton assistance.

Participants had limited experience with treadmill walking. For safety, they were instructed to lightly hold the handrail, which was instrumented with 3D force sensors. As handrail use could affect participants' propulsion, foot placement, or center-of-mass displacement, we discarded strides in which the mean total handrail force increased by more than 5% body weight from the No Exoskeleton condition. The average force exerted on the handrail by all subjects was 6.5 ± 0.8% BW (Table S II, Very High condition), which is approximately the weight of the arm (62) and less than the force exerted by hemiparetic individuals on canes (87).

Conclusion

This article demonstrates, for the first time, that a portable bilateral hip exoskeleton that simultaneously applies frontal- and sagittal-plane hip torque can significantly increase step width, margin of stability of the paretic and non-paretic limb, and non-paretic limb propulsion in eight individuals with hemiparesis. These metrics are critical components of stability and gait efficiency. The increase in the stability metrics is strongly correlated with the level of abduction torque. This work provides a foundation for future studies that intentionally alter propulsion or foot placement to improve gait efficiency and stability as needed to enhance mobility for hundreds of millions of individuals with hemiparesis.

List of abbreviations

AFO (ankle-foot orthosis), BW (body weight), CoM (center of mass), xCoM (extrapolated center of mass), ML (mediolateral), MDC (minimal detectable change), FAC (Functional Ambulation Category), TBI (traumatic brain injury)

Declarations

Ethics approval and consent to participate: Participants in the experiment provided written informed consent. The study protocol was approved by the University of Utah Institutional Review Board (Utah IRB #120712).

Consent for publication: Participants in the experiment consented to the dissemination and publication of photos and video material

Availability of data and materials: The datasets used and/or analyzed during the current study are available from the corresponding author on reasonable request.

Competing interests: The authors declare no competing interests.

Funding: This work was supported in part by the National Science Foundation under Award #2046287, in part by the Rocky Mountain Center for Occupational and Environmental Health CDC/NIOSH ERC under Grant T420H008414, and in part by the National Institutes of Health Training under Grant 1T32TR004394-01.

Authors contributions: DA designed the exoskeleton, control algorithm, and experimental protocol, and performed data collection and analysis, and prepared the manuscript. AG designed the experimental protocol, performed data collection and analysis, and contributed to manuscript revision. OW performed data collection and contributed to manuscript preparation and revision. YZ advised on statistical analysis. LG supervised the design of the exoskeleton. RM contributed to data collection and manuscript preparation, and coordinated manuscript revision. SE assisted with subject recruitment. KBF supervised the analysis of biomechanical data. TL supervised all aspects of the project and secured funding. DA and AG contributed equally to the publication.

Acknowledgments: The authors acknowledge the technical assistance provided by Kai Pruyn during the data collection and Greg Stoddard during statistical analysis.

Supplementary Materials

A. Exoskeleton Performance

The exoskeleton used in this study applied torque in both the frontal and sagittal planes (Fig. S 1). During all exoskeleton conditions, the exoskeleton applied an extension torque to the paretic and non-paretic limb (paretic: 0.078 ± 0.006 Nm/kg which occurred at 23.1 ± 1.7% of the gait cycle; non-paretic: 0.092 ± 0.007 Nm/kg which occurred at 27.6 ± 0.8% of the gait cycle). The exoskeleton also applied flexion torque during all exoskeleton conditions (paretic: 0.108 ± 0.013 Nm/kg which occurred at 64.4 ± 1.5 % of the gait cycle, non-paretic: 0.102 ± 0.009 Nm/kg which occurred at 68.6 ± 0.8% of the gait cycle). The maximum flexion angle was largest for the Sagittal condition (paretic: 40.2 ± 2.7°; non-paretic: 45.4 ± 3.0°) and smallest in the Very High condition (paretic: 31.6 ± 3.7°; non-paretic: 38.5 ± 4.0°). The maximum extension angle was largest in the Low condition (paretic: 14.1 ± 2.8°; non-paretic: 12.9 ± 4.9°) and smallest in the Very High condition (paretic: 7.0 ± 3.0°; non-paretic: 5.2 ± 5.2°).

Frontal-plane torques were set at a constant abduction level and smallest in the Sagittal condition (paretic: 0.0 ± 0.0 Nm/kg; non-paretic: 0.0 ± 0.0 Nm/kg) and largest in the Very High condition (paretic: 0.152 ± 0.001 Nm/kg; non-paretic: 0.150 ± 0.001 Nm/kg). Abductions torques decreased the exoskeleton average adduction angle, which was largest in the Sagittal condition (paretic: 12.5 ± 2.9°; non-paretic: 7.2 ± 2.0 °) and smallest (i.e. most abducted) in the Very High condition (paretic: -6.5 ± 3.4°; non-paretic: -13.9 ± 1.0° degrees adduction).

The table on the following page summarizes the exoskeleton behaviors

Table S I Summary of Exoskeleton Performance

		Experimental Conditions, Values are reported as mean ± standard error				
		Sagittal	Low	Med	High	Very High
Paretic Actuator	Mean Abduction Angle (°)	-12.5 ±2.9	-7.5 ±3.6	-2.9 ±3.8	1.5 ±3.7	5.9 ±3.4
	Mean Abduction Torque (Nm/kg)	0.000 ±0.000	0.051 ±0.000	0.084 ±0.001	0.118 ±0.001	0.152 ±0.001
	Max Sagittal (Flexion) Angle (°)	40.2 ±2.7	35.4 ±2.7	34.5 ±2.6	31.7 ±2.6	31.9 ±3.4
	Min. Sagittal (Extension) Angle (°)	11.2 ±2.4	14.1 ±2.8	11.4 ±2.4	9.8 ±2.7	7.2 ±3.0
	Max Sagittal (Flexion) Torque (Nm/kg)	0.108 ±0.012	0.100 ±0.010	0.095 ±0.009	0.095 ±0.007	0.101 ±0.010
	Min. Sagittal (Extension) Torque (Nm/kg)	0.074 ±0.005	0.078 ±0.006	0.074 ±0.006	0.073 ±0.006	0.077 ±0.007
Non-Paretic Actuator	Mean Abduction Angle (°)	-7.2 ±1.9	0.4 ±1.8	5.9 ±1.8	9.9 ±1.2	13.0 ±1.0
	Mean Abduction Torque (Nm/kg)	0.000 ±0.000	0.051 ±0.000	0.084 ±0.001	0.118 ±0.001	0.150 ±0.001
	Max Sagittal (Flexion) Angle (°)	45.4 ±3.0	39.1 ±4.4	36.9 ±3.7	35.9 ±5.1	38.7 ±3.8
	Min. Sagittal (Extension) Angle (°)	10.9 ±3.7	13.0 ±4.8	10.3 ±4.0	9.9 ±5.7	4.7 ±4.9
	Max Sagittal (Flexion) Torque (Nm/kg)	0.086 ±0.004	0.090 ±0.004	0.094 ±0.005	0.097 ±0.007	0.102 ±0.008

B. Main Outcome Measures and Center of Mass Displacement

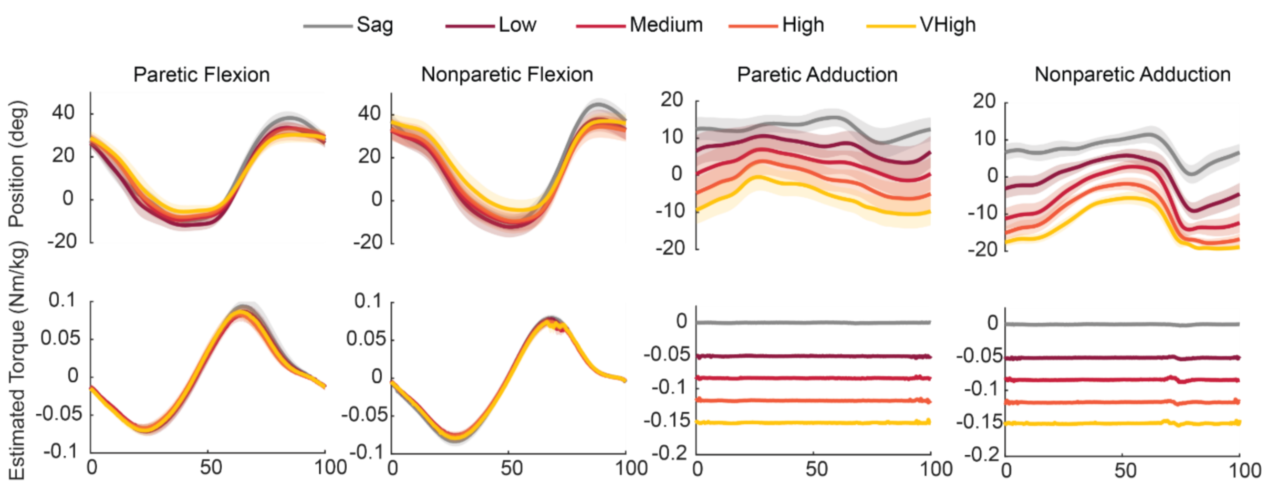

Fig. S 1 Exoskeleton (top) joint angle and (bottom) estimated torque for the paretic and non-paretic actuators segmented heel strike to heel strike. Hip flexion and hip adduction are positive. The plots show the condition means (solid lines) and standard error (shaded region).

The following table summarizes the main outcome measures and the center of mass and extrapolated center of mass mediolateral (ML) displacement.

Table S II Summary of Main Outcome Measures

		Experimental Conditions, Values are reported as mean ± standard erro					
		No Exo.	Sagittal	Low	Med	High	Very High
	Step Width (m)	0.126 ±0.022	0.127 ±0.024	0.147 ±0.017	0.158 ±0.020	0.166 ±0.020	0.180 ±0.02
	Center of Mass ML Displacement (m)	0.054 ±0.008	0.053 ±0.008	0.056 ±0.006	0.057 ±0.006	0.0567±0.007	0.058 ±0.00
	Extrapolated Center of Mass ML Displacement (m)	0.108 ±0.013	0.104 ±0.013	0.115 ±0.008	0.118 ±0.011	0.120 ±0.011	0.121 ±0.00
Paretic Limb	Margin of Stability, ML (m)	0.127 ±0.014	0.129 ±0.014	0.150 ±0.012	0.153 ±0.014	0.160 ±0.014	0.168 ±0.01
	Propulsion (% BW)	8.0 ±1.3	8.6 ±1.5	9.0 ±1.6	9.2 ±1.5	8.7 ±1.6	8.3 ±1
Non-Paretic Limb	Margin of Stability, ML (m)	0.091 ±0.006	0.097 ±0.009	0.103 ±0.007	0.106 ±0.007	0.109 ±0.007	0.112 ±0.00
	Propulsion (% BW)	14.5 ±1.6	15.4 ±1.8	16.3 ±1.9	16.3 ±1.8	16.6 ±1.9	17.0 ±1

Mediolateral (ML), and Body Weight (BW)

C. Kinematics and Kinetic Measures

The tables on the following pages summarize measures of the kinematics and kinetics for the 8 subjects and 6 experimental conditions.

Table S III Summary of *Paretic Limb* Kinematic and Kinetics

		Experimental Conditions, Values are reported as mean ± standard error					
		No Exo.	Sagittal	Low	Medium	High	Very High
Frontal-Plane Hip (Adduction Positive)	Mean Angle (°)	2.0 ±1.9	2.6 ±1.8	-0.4 ±1.8	-1.1 ±1.8	-1.6 ±2.0	-3.0 ±1.9
	Mean Torque (Nm/kg)	-0.265 ±0.025	-0.291 ±0.028	-0.182 ±0.024	-0.134 ±0.022	-0.098 ±0.027	-0.036 ±0.021
	Min. Torque (Nm/kg)	-0.675 ±0.057	-0.738 ±0.061	-0.571 ±0.046	-0.517 ±0.040	-0.491 ±0.056	-0.404 ±0.038
	Max Power (W/kg)	0.138 ±0.024	0.163 ±0.025	0.151 ±0.021	0.142 ±0.026	0.132 ±0.019	0.111 ±0.015
	Min. Power (W/kg)	-0.245 ±0.049	-0.277 ±0.038	-0.251 ±0.038	-0.237 ±0.063	-0.252 ±0.046	-0.209 ±0.034
	Total Positive Energy (J/kg)	0.033 ±0.006	0.042 ±0.008	0.037 ±0.008	0.033 ±0.009	0.029 ±0.006	0.024 ±0.005
Sagittal-Plane Hip (Flexion Positive)	Max Angle (°)	30.9 ±2.2	30.2 ±2.1	30.2 ±2.6	30.6 ±2.8	30.5 ±3.1	31.1 ±3.3
	Min. Angle (°)	-7.3 ±4.3	-9.2 ±4.1	-9.7 ±3.6	-8.5 ±3.9	-7.9 ±3.3	-6.7 ±3.8
	Max Torque (Nm/kg)	0.639 ±0.103	0.647 ±0.094	0.635 ±0.076	0.637 ±0.081	0.615 ±0.068	0.568 ±0.067
	Min Torque (Nm/kg)	-0.315 ±0.040	-0.313 ±0.044	-0.293 ±0.048	-0.293 ±0.034	-0.293 ±0.043	-0.283 ±0.029
	Max Power (W/kg)	0.723 ±0.154	0.711 ±0.142	0.674 ±0.120	0.654 ±0.124	0.635 ±0.127	0.588 ±0.112
	Min. Power (W/kg)	-0.387 ±0.096	-0.421 ±0.101	-0.452 ±0.116	-0.484 ±0.130	-0.394 ±0.095	-0.407 ±0.108
	Total Positive Energy (J/kg)	0.159 ±0.020	0.133 ±0.017	0.122 ±0.014	0.124 ±0.017	0.119 ±0.016	0.115 ±0.015
Sagittal-Plane Knee (Extension Positive)	Min. Stance Angle (°)	-9.5 ±3.4	-7.6 ±3.7	-8.9 ±3.0	-11.8 ±3.4	-13.0 ±3.6	-14.4 ±3.0
	Max Angle (°)	3.7 ±2.7	5.6 ±3.0	5.3 ±2.7	5.7 ±2.7	4.5 ±2.9	4.6 ±2.8
	Max Torque (Nm/kg)	0.284 ±0.065	0.296 ±0.062	0.283 ±0.060	0.325 ±0.069	0.362 ±0.078	0.361 ±0.085
	Min. Torque (Nm/kg)	-0.418 ±0.087	-0.473 ±0.086	-0.473 ±0.089	-0.505 ±0.087	-0.486 ±0.086	-0.480 ±0.081
	Max Power (W/kg)	0.385 ±0.049	0.405 ±0.042	0.381 ±0.040	0.452 ±0.039	0.447 ±0.056	0.474 ±0.043
	Min. Power (W/kg)	-0.584 ±0.118	-0.597 ±0.101	-0.559 ±0.107	-0.557 ±0.101	-0.554 ±0.110	-0.542 ±0.095
	Total Positive Energy (J/kg)	0.065 ±0.009	0.074 ±0.008	0.072 ±0.007	0.087 ±0.008	0.085 ±0.011	0.086 ±0.009
Sagittal-Plane Ankle (Dorsiflexion Positive)	Max Angle (°)	13.2 ±2.2	13.4 ±2.2	13.1 ±2.2	12.7 ±2.1	12.6 ±2.1	11.9 ±1.9
	Min. Angle (°)	-11.2 ±4.0	-11.7 ±4.1	-12.1 ±4.2	-11.3 ±4.2	-10.9 ±4.1	-10.5 ±4.1
	Max Torque (Nm/kg)	0.088 ±0.029	0.089 ±0.029	0.085 ±0.026	0.079 ±0.019	0.063 ±0.017	0.059 ±0.015
	Min. Torque (Nm/kg)	-1.032 ±0.070	-1.073 ±0.073	-1.054 ±0.078	-1.079 ±0.081	-1.066 ±0.082	-1.047 ±0.077
	Max Power (W/kg)	0.803 ±0.208	0.821 ±0.213	0.795 ±0.210	0.841 ±0.220	0.779 ±0.208	0.739 ±0.189
	Min. Power (W/kg)	-0.603 ±0.100	-0.661 ±0.123	-0.606 ±0.115	-0.594 ±0.100	-0.577 ±0.122	-0.508 ±0.096
	Total Positive Energy (J/kg)	0.085 ±0.022	0.086 ±0.024	0.085 ±0.024	0.095 ±0.028	0.086 ±0.025	0.085 ±0.024
Lower Limb	Positive Energy (J/kg)	0.343 ±0.041	0.336 ±0.038	0.316 ±0.038	0.339 ±0.047	0.320 ±0.040	0.309 ±0.040
Mean of Absolute Handrail Force	Resultant (%BW)	1.4 ±0.6	1.4 ±0.6	1.7 ±0.8	1.6 ±0.7	2.0 ±0.9	1.9 ±0.9
	X (%BW)	0.5 ±0.3	0.6 ±0.3	0.6 ±0.4	0.6 ±0.4	0.7 ±0.4	0.6 ±0.3
	Y (%BW)	0.3 ±0.1	0.3 ±0.1	0.4 ±0.1	0.4 ±0.1	0.4 ±0.2	0.4 ±0.2

Table S IV Summary of *Non-Paretic Limb* Kinematic and Kinetics

		Experimental Conditions, Values are reported as mean ± standard error					
		No Exo	Sagittal	Low	Medium	High	Very High
Frontal-Plane Hip (Adduction Positive)	Mean Angle (°)	1.1 ±1.3	-0.5 ±1.7	-2.3 ±1.5	-3.9 ±1.7	-4.4 ±1.6	-5.3 ±1.5
	Mean Torque (Nm/kg)	-0.425 ±0.028	-0.410 ±0.024	-0.364 ±0.033	-0.317 ±0.037	-0.289 ±0.041	-0.236 ±0.039
	Min. Torque (Nm/kg)	-0.948 ±0.046	-0.932 ±0.036	-0.884 ±0.056	-0.826 ±0.054	-0.768 ±0.068	-0.713 ±0.056
	Max Power (W/kg)	0.363 ±0.055	0.421 ±0.050	0.412 ±0.045	0.410 ±0.044	0.356 ±0.043	0.325 ±0.041
	Min. Power (W/kg)	-0.330 ±0.051	-0.378 ±0.043	-0.463 ±0.051	-0.488 ±0.059	-0.440 ±0.053	-0.392 ±0.048
	Total Positive Energy (J/kg)	0.054 ±0.009	0.063 ±0.010	0.066 ±0.004	0.057 ±0.003	0.053 ±0.005	0.050 ±0.005
Sagittal-Plane Hip (Extension Positive)	Max Angle (°)	37.3 ±2.8	38.7 ±3.1	36.7 ±2.4	38.0 ±2.7	37.1 ±2.1	37.4 ±2.4
	Min. Angle (°)	-9.0 ±3.4	-10.7 ±3.5	-12.0 ±2.7	-9.9 ±3.3	-11.2 ±2.6	-10.0 ±3.1
	Max Torque (Nm/kg)	0.540 ±0.113	0.575 ±0.103	0.555 ±0.085	0.509 ±0.098	0.534 ±0.083	0.523 ±0.072
	Min Torque (Nm/kg)	-0.614 ±0.058	-0.599 ±0.055	-0.553 ±0.057	-0.587 ±0.054	-0.563 ±0.063	-0.586 ±0.059
	Max Power (W/kg)	0.850 ±0.124	0.868 ±0.107	0.758 ±0.100	0.764 ±0.105	0.720 ±0.100	0.728 ±0.081
	Min. Power (W/kg)	-0.395 ±0.110	-0.403 ±0.099	-0.362 ±0.076	-0.321 ±0.084	-0.379 ±0.101	-0.375 ±0.084
	Total Positive Energy (J/kg)	0.269 ±0.044	0.246 ±0.048	0.225 ±0.050	0.232 ±0.048	0.224 ±0.044	0.225 ±0.042
Sagittal-Plane Knee (Flexion Positive)	Min. Stance Angle (°)	-18.2 ±2.9	-18.9 ±2.7	-21.6 ±2.8	-22.3 ±2.8	-23.1 ±2.6	-23.2 ±2.9
	Max Angle (°)	-2.5 ±3.2	-1.1 ±3.2	-1.4 ±3.2	-1.5 ±3.3	-1.6 ±3.1	-2.8 ±3.3
	Max Torque (Nm/kg)	0.424 ±0.068	0.495 ±0.085	0.540 ±0.094	0.544 ±0.091	0.548 ±0.106	0.518 ±0.097
	Min. Torque (Nm/kg)	-0.291 ±0.034	-0.333 ±0.042	-0.347 ±0.052	-0.355 ±0.058	-0.340 ±0.053	-0.330 ±0.049
	Max Power (W/kg)	0.459 ±0.100	0.626 ±0.116	0.643 ±0.128	0.709 ±0.135	0.680 ±0.142	0.628 ±0.119
	Min. Power (W/kg)	-0.900 ±0.098	-0.897 ±0.101	-0.933 ±0.099	-0.922 ±0.089	-0.855 ±0.085	-0.869 ±0.072
	Total Positive Energy (J/kg)	0.092 ±0.014	0.130 ±0.025	0.129 ±0.024	0.140 ±0.024	0.130 ±0.025	0.119 ±0.022
Sagittal-Plane Ankle (Dorsiflexion Positive)	Max Angle (°)	18.3 ±1.9	19.1 ±1.7	19.2 ±2.0	19.1 ±1.8	19.2 ±1.7	19.5 ±1.9
	Min. Angle (°)	-9.6 ±3.4	-10.3 ±3.3	-9.9 ±3.3	-8.6 ±3.3	-8.3 ±3.4	-8.1 ±3.3
	Max Torque (Nm/kg)	0.063 ±0.011	0.075 ±0.016	0.050 ±0.009	0.050 ±0.007	0.041 ±0.005	0.046 ±0.008
	Min. Torque (Nm/kg)	-1.347 ±0.073	-1.412 ±0.092	-1.417 ±0.077	-1.403 ±0.081	-1.396 ±0.074	-1.377 ±0.069
	Max Power (W/kg)	2.108 ±0.365	2.462 ±0.473	2.199 ±0.337	2.170 ±0.350	2.102 ±0.337	2.190 ±0.348
	Min. Power (W/kg)	-0.597 ±0.093	-0.739 ±0.083	-0.664 ±0.089	-0.678 ±0.096	-0.638 ±0.095	-0.620 ±0.100
	Total Positive Energy (J/kg)	0.219 ±0.038	0.262 ±0.060	0.236 ±0.036	0.225 ±0.037	0.225 ±0.039	0.228 ±0.038
Lower Limb	Positive Energy (J/kg)	0.634 ±0.036	0.702 ±0.073	0.656 ±0.037	0.655 ±0.043	0.633 ±0.031	0.622 ±0.035
Mean of	Resultant (%BW)	4.3 ±0.8	4.9 ±0.7	5.5 ±0.8	5.6 ±0.8	6.3 ±0.8	6.5 ±0.8

D. Supplementary Video

Please find a supplementary video, titled Additional File 1.mp4, in the additional files section.

References

1. Feigin VL, Brainin M, Norrving B, Martins SO, Pandian J, Lindsay P, et al. World Stroke Organization: Global Stroke Fact Sheet 2025. International Journal of Stroke. 2025 Feb 3;20(2):132–44. doi:10.1177/17474930241308142
2. Olney SJ, Richards C. Hemiparetic gait following stroke. Part I: Characteristics. Gait Posture. 1996 Apr;4(2):136–48. doi:10.1016/0966-6362(96)01063-6
3. Sheffler LR, Chae J. Hemiparetic Gait. Phys Med Rehabil Clin N Am. 2015 Nov;26(4):611–23. doi:10.1016/j.pmr.2015.06.006
4. Allen JL, Kautz SA, Neptune RR. Step length asymmetry is representative of compensatory mechanisms used in post-stroke hemiparetic walking. Gait Posture. 2011 Apr;33(4):538–43. doi:10.1016/j.gaitpost.2011.01.004
5. Balasubramanian CK, Bowden MG, Neptune RR, Kautz SA. Relationship Between Step Length Asymmetry and Walking Performance in Subjects With Chronic Hemiparesis. Arch Phys Med Rehabil. 2007 Jan;88(1):43–9. doi:10.1016/j.apmr.2006.10.004
6. Farris DJ, Hampton A, Lewek MD, Sawicki GS. Revisiting the mechanics and energetics of walking in individuals with chronic hemiparesis following stroke: from individual limbs to lower limb joints. J Neuroeng Rehabil. 2015 Dec 27;12(1):24. doi:10.1186/s12984-015-0012-x
7. Forster A, Young J. Incidence and consequences offalls due to stroke: a systematic inquiry. BMJ. 1995 Jul 8;311(6997):83–6. doi:10.1136/bmj.311.6997.83
8. Weerdesteyn V, Niet M de, van Duijnhoven HJR, Geurts ACH. Falls in individuals with stroke. The Journal of Rehabilitation Research and Development. 2008;45(8):1195. doi:10.1682/JRRD.2007.09.0145
9. Zamparo P, Francescato MP, De Luca G, Lovati L, di Prampera PE. The energy cost of level walking in patients with hemiplegia. Scand J Med Sci Sports. 1995 Dec 30;5(6):348–52. doi:10.1111/j.1600-0838.1995.tb00057.x
10. Platts MM, Rafferty D, Paul L. Metabolic cost of overground gait in younger stroke patients and healthy controls. Med Sci Sports Exerc. 2006 Jun;38(6):1041–6. doi:10.1249/01.mss.0000222829.34111.9c PubMed PMID: 16775542.
11. Lord SE, McPherson K, McNaughton HK, Rochester L, Weatherall M. Community ambulation after stroke: how important and obtainable is it and what measures appear predictive? Arch Phys Med Rehabil. 2004 Feb;85(2):234–9. doi:10.1016/j.apmr.2003.05.002
12. Combs SA, Van Puymbroeck M, Altenburger PA, Miller KK, Dierks TA, Schmid AA. Is walking faster or walking farther more important to persons with chronic stroke? Disabil Rehabil. 2013 May 5;35(10):860–7. doi:10.3109/09638288.2012.717575
13. Rand D, Eng JJ, Tang PF, Hung C, Jeng JS. Daily physical activity and its contribution to the health-related quality of life of ambulatory individuals with chronic stroke. Health Qual Life Outcomes. 2010 Dec 3;8(1):80. doi:10.1186/1477-7525-8-80
14. Shavelle RM, Brooks JC, Strauss DJ, Turner-Stokes L. Life Expectancy after Stroke Based On Age, Sex, and Rankin Grade of Disability: A Synthesis. Journal of Stroke and Cerebrovascular Diseases. 2019 Dec;28(12):104450. doi:10.1016/j.jstrokecerebrovasdis.2019.104450

15. Jonkers I, Delp S, Patten C. Capacity to increase walking speed is limited by impaired hip and ankle power generation in lower functioning persons post-stroke. Gait Posture. 2009 Jan;29(1):129–37. doi:10.1016/j.gaitpost.2008.07.010
16. Cruz TH, Lewek MD, Dhaher YY. Biomechanical impairments and gait adaptations post-stroke: Multi-factorial associations. J Biomech. 2009 Aug;42(11):1673–7. doi:10.1016/j.jbiomech.2009.04.015
17. Peterson CL, Cheng J, Kautz SA, Neptune RR. Leg extension is an important predictor of paretic leg propulsion in hemiparetic walking. Gait Posture. 2010 Oct;32(4):451–6. doi:10.1016/j.gaitpost.2010.06.014
18. Riley PO, Croce U Della, Casey Kerrigan D. Propulsive adaptation to changing gait speed. J Biomech. 2001 Feb;34(2):197–202. doi:10.1016/S0021-9290(00)00174-3
19. Ellis RG, Sumner BJ, Kram R. Muscle contributions to propulsion and braking during walking and running: Insight from external force perturbations. Gait Posture. 2014 Sep;40(4):594–9. doi:10.1016/j.gaitpost.2014.07.002
20. Hsiao HY, Zabielski TM, Palmer JA, Higginson JS, Binder-Macleod SA. Evaluation of measurements of propulsion used to reflect changes in walking speed in individuals poststroke. J Biomech. 2016 Dec 8;49(16):4107–12. doi:10.1016/j.jbiomech.2016.10.003 PubMed PMID: 27756571.
21. Hsiao HaoYuan, Awad Louis N, Palmer Jacqueline A, Higginson Jill S, Binder-Macleod Stuart A. Contribution of Paretic and Nonparetic Limb Peak Propulsive Forces to Changes in Walking Speed in Individuals Poststroke. Neurorehabil Neural Repair. 2015 Dec 31;30(8):743–52. doi:10.1177/1545968315624780
22. Detrembleur C, Dierick F, Stoquart G, Chantraine F, Lejeune T. Energy cost, mechanical work, and efficiency of hemiparetic walking. Gait Posture. 2003 Oct;18(2):47–55. doi:10.1016/S0966-6362(02)00193-5
23. Hesse S, Werner C, Paul T, Bardeleben A, Chaler J. Influence of walking speed on lower limb muscle activity and energy consumption during treadmill walking of hemiparetic patients. Arch Phys Med Rehabil. 2001 Nov;82(11):1547–50. doi:10.1053/apmr.2001.26607
24. Awad LN, Knarr BA, Kudzia P, Buchanan TS. The Interplay Between Walking Speed, Economy, and Stability After Stroke. Journal of Neurologic Physical Therapy. 2023 Apr;47(2):75–83. doi:10.1097/NPT.0000000000000431
25. MacKinnon CD, Winter DA. Control of whole body balance in the frontal plane during human walking. J Biomech. 1993 Jun;26(6):633–44. doi:10.1016/0021-9290(93)90027-C
26. Horak FB. Postural orientation and equilibrium: what do we need to know about neural control of balance to prevent falls? Age Ageing. 2006 Sep 1;35(suppl_2):ii7–11. doi:10.1093/ageing/afl077
27. de Kam D, Roelofs JMB, Bruijnes AKBD, Geurts ACH, Weerdesteyn V. The Next Step in Understanding Impaired Reactive Balance Control in People With Stroke: The Role of Defective Early Automatic Postural Responses. Neurorehabil Neural Repair. 2017 Aug 8;31(8):708–16. doi:10.1177/1545968317718267
28. de Haart M, Geurts AC, Huidekoper SC, Fasotti L, van Limbeek J. Recovery of standing balance in postacute stroke patients: a rehabilitation cohort study11No commercial party having a direct financial interest in the results of the research supporting this article has or will confer a benefit upon the authors(s) or upo. Arch Phys Med Rehabil. 2004 Jun;85(6):886–95. doi:10.1016/j.apmr.2003.05.012
29. Gray VL, Yang CL, McCombe Waller S, Rogers MW. Lateral Perturbation-Induced Stepping: Strategies and Predictors in Persons Poststroke. Journal of Neurologic Physical Therapy. 2017 Oct 1;41(4):222–8. doi:10.1097/NPT.0000000000000202 PubMed PMID: 28922313.

30. Cruz TH, Dhaher YY. Evidence of abnormal lower-limb torque coupling after stroke: An isometric study. Stroke. 2008;39(1):139–47. doi:10.1161/STROKEAHA.107.492413
31. Buesing C, Fisch G, O'Donnell M, Shahidi I, Thomas L, Mummidisetty CK, et al. Effects of a wearable exoskeleton stride management assist system (SMA®) on spatiotemporal gait characteristics in individuals after stroke: A randomized controlled trial. J Neuroeng Rehabil. 2015;12(1):1–14. doi:10.1186/s12984-015-0062-0 PubMed PMID: 26289955.
32. Murray SA, Ha KH, Hartigan C, Goldfarb M. An Assistive Control Approach for a Lower-Limb Exoskeleton to Facilitate Recovery of Walking Following Stroke. IEEE Transactions on Neural Systems and Rehabilitation Engineering. 2015 May;23(3):441–9. doi:10.1109/TNSRE.2014.2346193
33. Jayaraman A, O'Brien MK, Madhavan S, Mummidisetty CK, Roth HR, Hohl K, et al. Stride management assist exoskeleton vs functional gait training in stroke. Neurology. 2019 Jan 15;92(3). doi:10.1212/WNL.0000000000006782
34. Lee HJ, Lee SH, Seo K, Lee M, Chang WH, Choi BO, et al. Training for Walking Efficiency With a Wearable Hip-Assist Robot in Patients With Stroke. Stroke. 2019 Dec;50(12):3545–52. doi:10.1161/STROKEAHA.119.025950
35. Livolsi C, Conti R, Guanziroli E, Friðriksson Þ, Alexandersson Á, Kristjánsson K, et al. An impairment-specific hip exoskeleton assistance for gait training in subjects with acquired brain injury: a feasibility study. Sci Rep. 2022 Nov 11;12(1):19343. doi:10.1038/s41598-022-23283-w
36. Sawicki GS, Beck ON, Kang I, Young AJ, Simpson CS, Welker CG, et al. The exoskeleton expansion: Improving walking and running economy. J Neuroeng Rehabil. 2020;17(1):1–9. doi:10.1186/s12984-020-00663-9
37. Fang Y, Lerner ZF. Bilateral vs. Paretic-Limb-Only Ankle Exoskeleton Assistance for Improving Hemiparetic Gait: A Case Series. IEEE Robot Autom Lett. 2022 Apr;7(2):1246–53. doi:10.1109/LRA.2021.3139540
38. Pruyn K, Murray R, Gabert L, Lenzi T. Autonomous Powered Ankle Exoskeleton Improves Foot Clearance and Knee Hyperextension After Stroke: A Case Study. IEEE Trans Med Robot Bionics. 2025 Feb;7(1):51–8. doi:10.1109/TMRB.2024.3503893
39. Awad LN, Bae J, O'Donnell K, De Rossi SMM, Hendron K, Sloot LH, et al. A soft robotic exosuit improves walking in patients after stroke. Sci Transl Med. 2017 Jul 26;9(400):eaai9084. doi:10.1126/scitranslmed.aai9084
40. Sarkisian S V., Gunnell AJ, Bo Foreman K, Lenzi T. Knee Exoskeleton Reduces Muscle Effort and Improves Balance During Sit-to-Stand Transitions After Stroke: A Case Study. In: 2022 International Conference on Rehabilitation Robotics (ICORR). IEEE; 2022. p. 1–6. doi:10.1109/ICORR55369.2022.9896571
41. Chang CK, Lee C, Nuckols RW, Eckert-Erdheim A, Orzel D, Herman M, et al. Implementation of a unilateral hip flexion exosuit to aid paretic limb advancement during inpatient gait retraining for individuals post-stroke: a feasibility study. J Neuroeng Rehabil. 2024 Jul 18;21(1):121. doi:10.1186/s12984-024-01410-0
42. Pan YT, Kang I, Joh J, Kim P, Herrin KR, Kesar TM, et al. Effects of Bilateral Assistance for Hemiparetic Gait Post-Stroke Using a Powered Hip Exoskeleton. Ann Biomed Eng. 2023 Feb 1;51(2):410–21. doi:10.1007/s10439-022-03041-9 PubMed PMID: 35963920.
43. Livolsi C, Conti R, Ciapetti T, Guanziroli E, Fridriksson T, Alexandersson Á, et al. Bilateral hip exoskeleton assistance enables faster walking in individuals with chronic stroke-related gait impairments. Sci Rep. 2025;15(1):2017. doi:10.1038/s41598-025-86343-x
44. Archangeli D, Ishmael MK, Lenzi T. Assistive Powered Hip Exoskeleton Improves Self-Selected Walking Speed in One Individual with Hemiparesis: A Case Study. In: 2022

International Conference on Rehabilitation Robotics (ICORR). 2022. p. 1–6. doi:10.1109/ICORR55369.2022.9896568
45. Herrin K, Upton E, Young A. Towards meaningful community ambulation in individuals post stroke through use of a smart hip exoskeleton: A preliminary investigation. Assistive Technology. 2024 May 3;36(3):198–208. doi:10.1080/10400435.2023.2239555
46. Archangeli D, Ortolano B, Murray R, Gabert L, Lenzi T. A Lightweight Powered Hip Exoskeleton With Parallel Actuation for Frontal and Sagittal Plane Assistance. IEEE Transactions on Robotics. 2025;41:1711–27. doi:10.1109/TRO.2025.3539172
47. Alili A, Fleming A, Nalam V, Liu M, Dean J, Huang H. Abduction/Adduction Assistance From Powered Hip Exoskeleton Enables Modulation of User Step Width During Walking. IEEE Trans Biomed Eng. 2023;1–9. doi:10.1109/TBME.2023.3301444
48. Alili A, Nalam V, Tacca JR, Liu M, Si J, Huang H (Helen). Towards Advancing Mediolateral Balance by Hip Exoskeletons: A Reinforcement Learning-Based Approach for Proactive Step Width Control. 2025. doi:10.36227/techrxiv.174495359.94732664/v1
49. Leestma JK, Mathur S, Anderton MD, Sawicki GS, Young AJ. Dynamic Duo: Design and Validation of an Autonomous Frontal and Sagittal Actuating Hip Exoskeleton for Balance Modulation During Perturbed Locomotion. IEEE Robot Autom Lett. 2024 May;9(5):3995–4002. doi:10.1109/LRA.2024.3371290
50. Archangeli D, Ortolano B, Murray R, Gabert L, Lenzi T. Design and Evaluation of a Powered Hip Exoskeleton for Frontal and Sagittal Plane Assistance. In: 2024 10th IEEE RAS/EMBS International Conference for Biomedical Robotics and Biomechatronics (BioRob). IEEE; 2024. p. 1126–31. doi:10.1109/BioRob60516.2024.10719876
51. Ishmael MK, Archangeli D, Lenzi T. A Powered Hip Exoskeleton With High Torque Density for Walking, Running, and Stair Ascent. IEEE/ASME Transactions on Mechatronics. 2022 Dec 1;27(6):4561–72. doi:10.1109/TMECH.2022.3159506
52. Sarkisian S V., Ishmael MK, Hunt GR, Lenzi T. Design, Development, and Validation of a Self-Aligning Mechanism for High-Torque Powered Knee Exoskeletons. IEEE Trans Med Robot Bionics. 2020 May;2(2):248–59. doi:10.1109/tmrb.2020.2981951
53. Sarkisian S V., Ishmael MK, Lenzi T. Self-Aligning Mechanism Improves Comfort and Performance With a Powered Knee Exoskeleton. IEEE Transactions on Neural Systems and Rehabilitation Engineering. 2021;29:629–40. doi:10.1109/TNSRE.2021.3064463
54. Hood S, Ishmael MK, Gunnell A, Foreman KB, Lenzi T. A kinematic and kinetic dataset of 18 above-knee amputees walking at various speeds. Sci Data. 2020 May 21;7(1):150. doi:10.1038/s41597-020-0494-7
55. Taylor WR, Kornaropoulos EI, Duda GN, Kratzenstein S, Ehrig RM, Arampatzis A, et al. Repeatability and reproducibility of OSSCA, a functional approach for assessing the kinematics of the lower limb. Gait Posture. 2010 Jun;32(2):231–6. doi:10.1016/j.gaitpost.2010.05.005
56. Ehrig RM, Taylor WR, Duda GN, Heller MO. A survey of formal methods for determining functional joint axes. J Biomech. 2007 Jan;40(10):2150–7. doi:10.1016/j.jbiomech.2006.10.026
57. Pruyn K, Murray R, Gabert L, Foreman KB, Lenzi T. Portable hip exoskeleton improves walking economy for stroke survivors. Nature Communications 2026. 2026 Feb 14. doi:10.1038/s41467-026-69580-0
58. Winter DA. Biomechanics and Motor Control of Human Movement. 2nd ed. Hoboken, NJ: Wiley; 1990. 386 p.
59. Farris DJ, Sawicki GS. Linking the mechanics and energetics of hopping with elastic ankle exoskeletons. J Appl Physiol. 2012 Dec 15;113(12):1862–72. doi:10.1152/japplphysiol.00802.2012

60. Collins SH, Bruce Wiggin M, Sawicki GS. Reducing the energy cost of human walking using an unpowered exoskeleton. Nature. 2015;522(7555):212–5. doi:10.1038/nature14288
61. Ishmael MK, Gunnell A, Pruyn K, Creveling S, Hunt G, Hood S, et al. Powered Hip Exoskeleton Reduces Residual Hip Effort Without Affecting Kinematics and Balance in Individuals With Above-Knee Amputations During Walking. IEEE Trans Biomed Eng. 2023 Apr;70(4):1162–71. doi:10.1109/TBME.2022.3211842
62. Plagenhoef S, Evans FG, Abdelnour T. Anatomical Data for Analyzing Human Motion. Res Q Exerc Sport. 1983 Jun;54(2):169–78. doi:10.1080/02701367.1983.10605290
63. Kubinski SN, McQueen CA, Sittloh KA, Dean JC. Walking with wider steps increases stance phase gluteus medius activity. Gait Posture. 2015 Jan;41(1):130–5. doi:10.1016/j.gaitpost.2014.09.013
64. Hof AL, Gazendam MGJ, Sinke WE. The condition for dynamic stability. J Biomech. 2005 Jan;38(1):1–8. doi:10.1016/j.jbiomech.2004.03.025
65. Lewek MD, Sawicki GS. Trailing limb angle is a surrogate for propulsive limb forces during walking post-stroke. Clinical Biomechanics. 2019;67:115–8. doi:https://doi.org/10.1016/j.clinbiomech.2019.05.011
66. Ingraham KA, Remy CD, Rouse EJ. The role of user preference in the customized control of robotic exoskeletons. Sci Robot. 2022 Mar 30;7(64). doi:10.1126/scirobotics.abj3487
67. Kim J, Quinlivan BT, Deprey LA, Arumukhom Revi D, Eckert-Erdheim A, Murphy P, et al. Reducing the energy cost of walking with low assistance levels through optimized hip flexion assistance from a soft exosuit. Sci Rep. 2022 Jun 29;12(1):11004. doi:10.1038/s41598-022-14784-9
68. Sankoh AJ, Huque MF, Dubey SD. Some comments on frequently used multiple endpoint adjustment methods in clinical trials. Stat Med. 1997 Nov 30;16(22):2529–42. doi:10.1002/(SICI)1097-0258(19971130)16:22<2529::AID-SIM692>3.0.CO;2-J
69. Wilson GT. Time Series Analysis: Forecasting and Control, 5th Edition, by George E. P. Box, Gwilym M. Jenkins, Gregory C. Reinsel and Greta M. Ljung, 2015. Published by John Wiley and Sons Inc., Hoboken, New Jersey, pp. 712. ISBN: 978-1-118-67502-1. J Time Ser Anal. 2016 Sep 27;37(5):709–11. doi:10.1111/jtsa.12194
70. Luu TP, He Y, Nakagome S, Nathan K, Brown S, Gorges J, et al. Multi-Trial Gait Adaptation of Healthy Individuals during Visual Kinematic Perturbations. Front Hum Neurosci. 2017 Jun 20;11. doi:10.3389/fnhum.2017.00320
71. Watson F, Fino PC, Thornton M, Heracleous C, Loureiro R, Leong JJH. Use of the margin of stability to quantify stability in pathologic gait – a qualitative systematic review. BMC Musculoskelet Disord. 2021 Dec 28;22(1):597. doi:10.1186/s12891-021-04466-4
72. McAndrew Young PM, Dingwell JB. Voluntarily changing step length or step width affects dynamic stability of human walking. Gait Posture. 2012 Mar;35(3):472–7. doi:10.1016/j.gaitpost.2011.11.010
73. Herssens N, van Criekinge T, Saeys W, Truijen S, Vereeck L, van Rompaey V, et al. An investigation of the spatio-temporal parameters of gait and margins of stability throughout adulthood. J R Soc Interface. 2020 May 20;17(166):20200194. doi:10.1098/rsif.2020.0194
74. Hof AL, van Bockel RM, Schoppen T, Postema K. Control of lateral balance in walking. Experimental findings in normal subjects and above-knee amputees. Gait Posture. 2007;25(2):250–8. doi:10.1016/j.gaitpost.2006.04.013 PubMed PMID: 16740390.

75. Roerdink M, Lamoth CJ, Kwakkel G, van Wieringen PC, Beek PJ. Gait Coordination After Stroke: Benefits of Acoustically Paced Treadmill Walking. Phys Ther. 2007 Aug 1;87(8):1009–22. doi:10.2522/ptj.20050394
76. Peebles AT, Reinholdt A, Bruetsch AP, Lynch SG, Huisinga JM. Dynamic margin of stability during gait is altered in persons with multiple sclerosis. J Biomech. 2016 Dec;49(16):3949–55. doi:10.1016/j.jbiomech.2016.11.009
77. Chen G, Patten C, Kothari DH, Zajac FE. Gait differences between individuals with post-stroke hemiparesis and non-disabled controls at matched speeds. Gait Posture. 2005 Aug;22(1):51–6. doi:10.1016/j.gaitpost.2004.06.009 PubMed PMID: 15996592.
78. Hak L, Houdijk H, Van Der Wurff P, Prins MR, Mert A, Beek PJ, et al. Stepping strategies used by post-stroke individuals to maintain margins of stability during walking. Clinical Biomechanics. 2013;28(9–10):1041–8. doi:10.1016/j.clinbiomech.2013.10.010
79. McAndrew Young PM, Wilken JM, Dingwell JB. Dynamic margins of stability during human walking in destabilizing environments. J Biomech. 2012 Apr;45(6):1053–9. doi:10.1016/j.jbiomech.2011.12.027
80. Zhang T, Tran M, Huang H. Design and experimental verification of hip exoskeleton with balance capacities for walking assistance. IEEE/ASME Transactions on Mechatronics. 2018;23(1):274–85. doi:10.1109/TMECH.2018.2790358
81. Park J, Nam K, Yun J, Moon J, Ryu J, Park S, et al. Effect of hip abduction assistance on metabolic cost and balance during human walking. Sci Robot. 2023 Oct 25;8(83). doi:10.1126/scirobotics.ade0876
82. Mooney LM, Herr HM. Biomechanical walking mechanisms underlying the metabolic reduction caused by an autonomous exoskeleton. J Neuroeng Rehabil. 2016;13(1):1–12. doi:10.1186/s12984-016-0111-3
83. Jackson RW, Collins SH. An experimental comparison of the relative benefits of work and torque assistance in ankle exoskeletons. J Appl Physiol. 2015 Sep 1;119(5):541–57. doi:10.1152/japplphysiol.01133.2014
84. Cooper A, Alghamdi GA, Alghamdi MA, Altowaijri A, Richardson S. The Relationship of Lower Limb Muscle Strength and Knee Joint Hyperextension during the Stance Phase of Gait in Hemiparetic Stroke Patients. Physiotherapy Research International. 2012 Sep 7;17(3):150–6. doi:10.1002/pri.528
85. Geerars M, Minnaar-van der Feen N, Huisstede BMA. Treatment of knee hyperextension in post-stroke gait. A systematic review. Gait Posture. 2022 Jan;91:137–48. doi:10.1016/j.gaitpost.2021.08.016
86. Tani Y, Otaka Y, Kudo M, Kurayama T, Kondo K. Prevalence of Genu Recurvatum during Walking and Associated Knee Pain in Chronic Hemiplegic Stroke Patients: A Preliminary Survey. Journal of Stroke and Cerebrovascular Diseases. 2016 May;25(5):1153–7. doi:10.1016/j.jstrokecerebrovasdis.2016.01.028
87. Murray MP, Seireg AH, Scholz RC. A Survey Of The Time, Magnitude And Orientation Of Forces Applied To Walking Sticks By Disabled Men. Am J Phys Med. 1969;48(1):1–13.